Available online at www.CivileJournal.org

Civil Engineering Journal

Vol. 3, No. 1, January, 2017

Seismic Response Reduction of Steel MRF Using SMA Equipped Innovated Low-damage Column Foundation Connection

R. Jamalpour [a], M. Nekooei [a*], A. Sarvghad Moghadam [b]

[a] *Department of Civil Engineering, Science and Research Branch, Islamic Azad University, Tehran, Iran.*

[b] *International Institute of Earthquake Engineering and Seismology (IIEES), Tehran, Iran.*

Received 17 December 2016; Accepted 22 January 2017

Abstract

Connections in MRFs are the most important members and seismic behaviour is affected by function of beam column connections as well as column foundation connections. If the connections are able to provide the required ductility and efficiency against the seismic excitation, the seismic capacity of the MRF performed by these connections will be affected. SMAs have recently been used as a tool to dissipate energy in structures. So far, using of them for column foundation connections has been applied much less. In this paper, SMAs have been introduced and an innovated column foundation connection equipped with SMA has been suggested. Micro and macro behaviour of the connection has been studied and it was applied in sample MRF. Seismic response of the MRF under different earthquakes by equipping the connection with steels/SMAs bars have been studied and compared. Finally, results indicated that MRF with this connection showed proper seismic performance.

Keywords: Seismic Performance; Low-damage Column; Foundation Connections; Steel MRF; NiTi SMA.

1. Introduction

One of the resistant structures against lateral loads is moment resistant frame (MRF) in which the beams and columns form a moment frame through a fixed support in connections. Connections are the most important members in MRFs. Because of this importance, recently many researchers focused their investigation on beam to column connection and behaviour of MRFs. Experimental results of three Reduced Beam Section Tubular TW-RBS connections under cyclic loading have been conducted [1]. The load transfer mechanism and load-bearing capacity of cast steel joints for H-shaped beam to square tube column connection based on the deformation compatibility theory are studied [2]. The optimum design of planar frames with semi-rigid connections by standard sections from (AISC) table has been Studied [3]. Steel bolted connection and bolts satiation on connection plate for high strength steel connections built up with high strength bolts have been investigated [4].

The performance and ductility capacity of the connections in bending structures are the most crucial factors governing the seismic capacity of these structures. In addition to beam-column connections, the method of connecting the columns to foundations is of great importance in tolerating lateral loads by the MRFs. Different ways of connecting column to foundation brings about different performance of MRFs. Since the connecting method of column to foundation was decided by the designer, one can decide on frame performance selection. This issue can be the basis for offering a controlled connection method, the schematic of which has been shown in Figure 1. If the above mentioned connection has an unlimited rotational stiffness, it will function like a restraining connection; if it lacks a rotational stiffness, it will perform like a hinged connection and in the aforementioned scope, it will show appropriate performance under rotational and seismic loadings if it applies appropriate materials. The dynamic performance of the

* Corresponding author: msnekooei@gmail.com

controlled connection requires high elasticity, great strains toleration, energy dissipation, resilience. Having applied the required plans in the connection, one can improve the stiffness, lateral ductility of steel moment frames (energy dissipation capability arising from seismic stimulations), and quake removing elements (kinds, stiffness, mortality). Thus, dynamic controlled performance of these connections calls for using special materials which are referred to as SMAs.

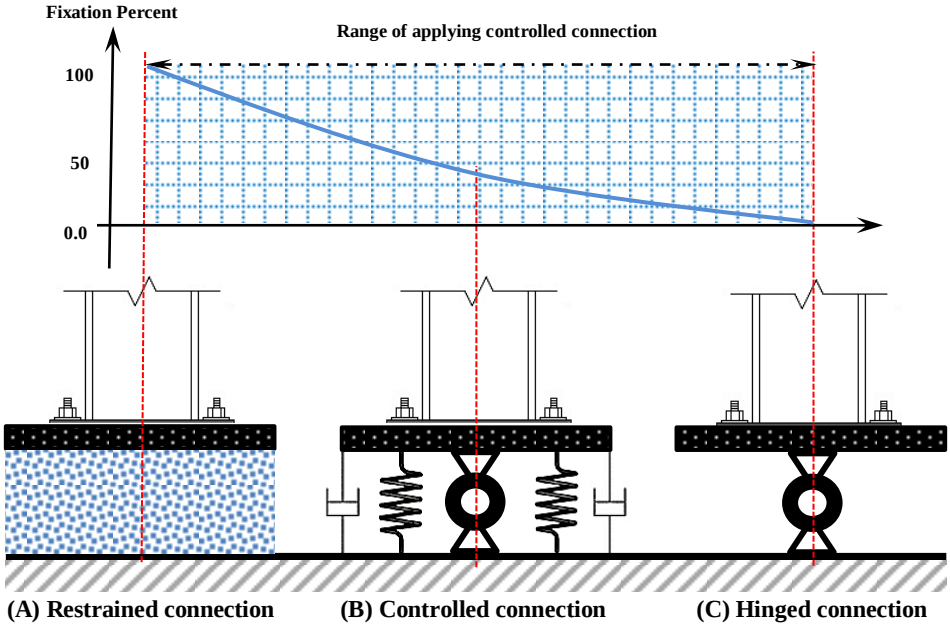

Figure 1. Schematic of different kinds of column foundation connections and its application scope

2. Introducing the Shape Memory Alloy (SMA) and Its Behavior

Shape memory alloys (SMAs) are exotic materials with magical properties under visible permanent deformations by up to 10% or more. In addition, they entail metallic properties such as strength, stiffness, high expenditure, cast ability and so on [5]. In recent decades, a great deal of research in civil engineering and structural engineering have been focused on using intelligent systems in civil development projects with an emphasis on structural response control against vibration and seismic waves. Many innovative tools and systems have been proposed mainly using shape memory alloys based on Nitinol and copper so as to absorb some of the energy loss caused by earthquakes and dampen the earthquake forces aimed at structural retrofitting. Shape memory alloys have two outstanding features including a shape memory and superelastic behavior. The shape memory alloys are capable of bouncing back to a preset shape when heating up over the characteristic temperature of austenite transformation (Af). They are also capable of high strain recovery (about 8%).

2.1. Superelastic and Shape memory Effect of SMAs

The stress-strain hysteresis due to mechanical loading-unloading under isothermal conditions is known as superelastic effect. Figure 2. illustrates the conventional shape memory effect on path (1 to 6) and the superelastic effect on path (7 to 13) on temperature-stress-strain diagram [6]. In response to superelastic shape memory alloys, the phase transformations lead to nonlinear hysteresis reaction. This has given such materials superior properties in energy dissipation as an excellent option for damper materials.

2.2. Austenite and Martensite Phase of SMAs

Because of different crystal structures of austenite and martensite, the SMAs lead to different superelastic responses in various parts, being sensitive to operating temperature. Figure 3. displays the performance of a superelastic wire sample at different temperatures. The classic Nitinol superelastic wires and rods are among SMA applicable in structural connections as adopted in the current paper. Many innovative tools and systems have been proposed mainly using SMAs based on Nitinol and copper so as to absorb some of the energy dissipation caused by earthquakes and damping the earthquake forces aimed at structural retrofitting. The variable stiffness in superelastic behavior can be used to control the force and displacement in three different strain scenarios. At strains lower than 1%, the austenite modulus of elasticity can be employed to limit the strains. In the middle strain levels more than 1% and less than 6%, the reduced modulus can be used to limit the force transferred to the structure, even if there is a large displacement. In

large strains more than 6%, the increased modulus in stress induced martensitic phase can be used to control displacement under earthquake induced stress conditions. By the load removal, the low-stress path in reverse transfer leads to the hysteresis energy loss, which is a desirable feature control the vibrations exerted on structures. Furthermore, the superelastic behavior provides the use of austenite elements to self-centering property of SMAs. In fact, they obtain the original shape after deformation caused by stress or temperature.

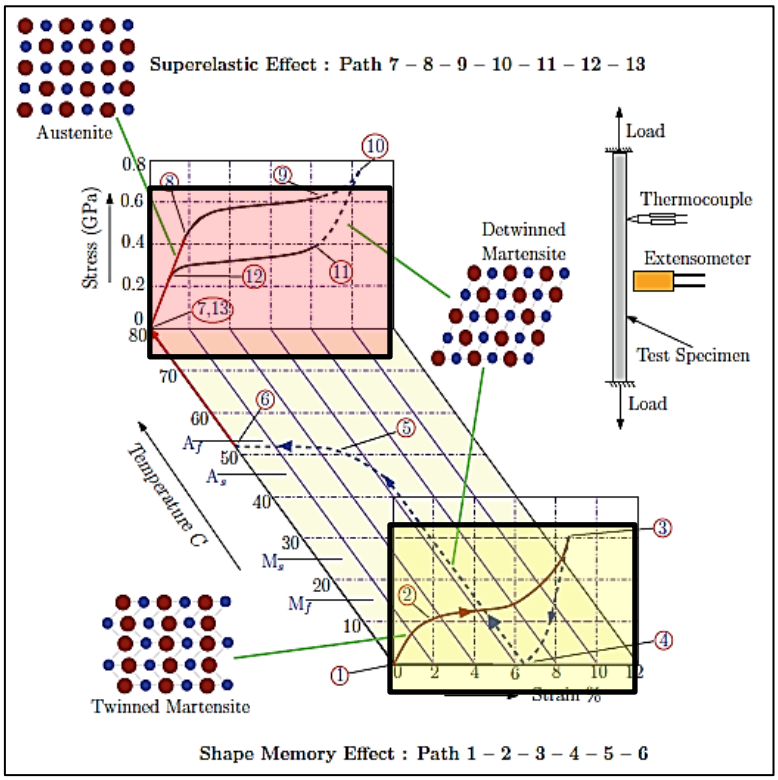

Shape memory effect (Path 1-6) and superelastic effect (Path 7-13) can be seen. This reversibility effect is a manifestation of solid-phase transformations between a stable austenitic phase, high-temperature phase and low-temperature martensitic phase**.**

Figure 2. Three-dimensional temperature-stress-strain diagram describing a thermo-mechanical test

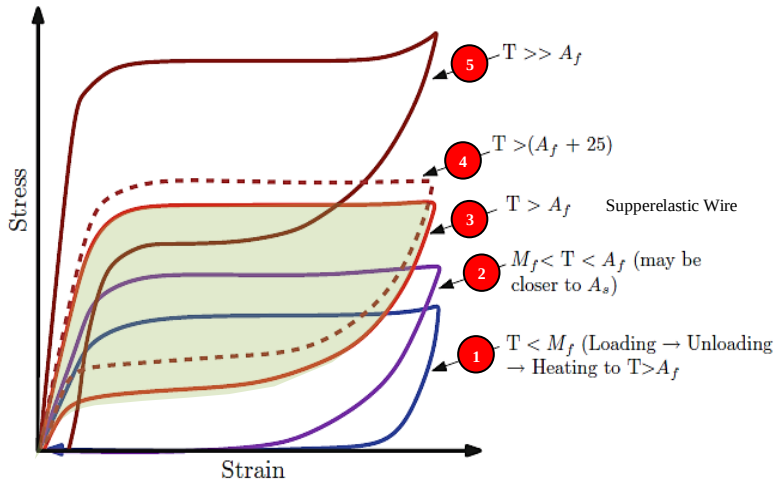

Curve (1) The Response of the wire under the influence of temperature lower than Mf after it was unloaded and achieved zero stress. The shape memory property was achieved by heating the wire above the A_f.
Curve (2) The response of the wire above the temperature M_f<T<A_f, which is almost identical to A_s.
Curve (3) Displays the classic superelastic wire above A_f.
Curve (4) Displays the temperature-dependent superelastic wire.
Curve (5) The response of the temperatures far higher than A_f.

Figure 3. Response of SMA wire under different temperature regimes

3. Review of Related Literature on SMAs Application in Steel Structures Connections

The application of SMAs in structure has been long highlighted. Application of SMA in tuned mass dampers to reduce the reaction of wide span steel frames has been studied [7]. General applications of SMA in structures have been introduced [8]. Generally speaking, after the 1994 Northridge earthquake numerous studies have been done on reinforcing the connections against the earthquake. Quite a few researchers have suggested using systems of SMAs due to their potential in creating a simple ductile self-centering mechanism as well as their unique capability in strain self-centering up to %8 to control the frequency reaction of connections under high earthquake vibrations especially in steel structures. Experimental testing on beam column connections in real scale with/without using Nitinol tendons have been reported [9]. The shape memory effect has been tested in steel beam column connection using a Nitinol SMA under semi static loading. This connection includes four NiTi SMA rods which connected the upper and lower beam flanges to column flange and functioned as a primary torque conveyance mechanism [10]. Some studies on connection sample with a primary strain using four 3^{mm} copper-aluminum-beryllium SMA rods have been done. The suggested structure with end plate connection between a structural hollow beam and wide flange steel column. SMA rods in austenite phase were used to reinforce the end plate on the column flange. Experimental testing indicated that beam column connection did not bring about a considerable a superelastic performance, balanced energy dissipation level, and strength drawdown after being exposed to numerous rotations up to %3 of relative displacement [11]. Some comparative studies on internal beam column connections, Figure 4. have been studied. In which steel tendons , Nitinol martensite SMAs and superelastic Nitinol SMAs and aluminum, used. Superelastic SMA connections can recover %85 of their original shape after the relative displacement of %5 which made it possible to concentrate all the non-elastic displacement on the tendons while other parts of the connection were in an elastic state [12].

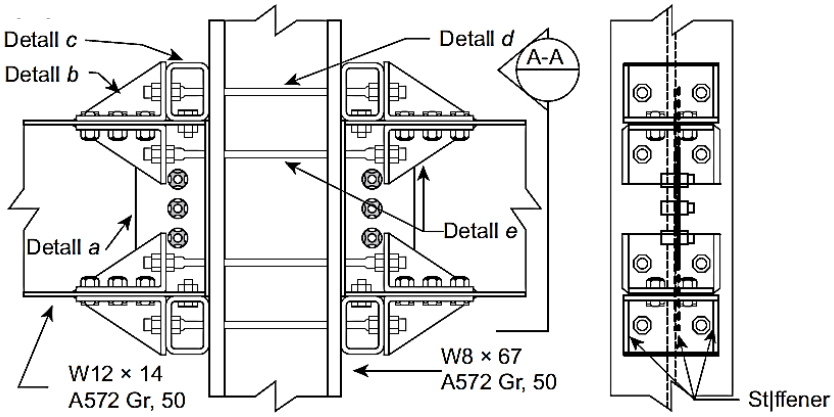

Figure 4. Beam column connection in the experiment done by [11]

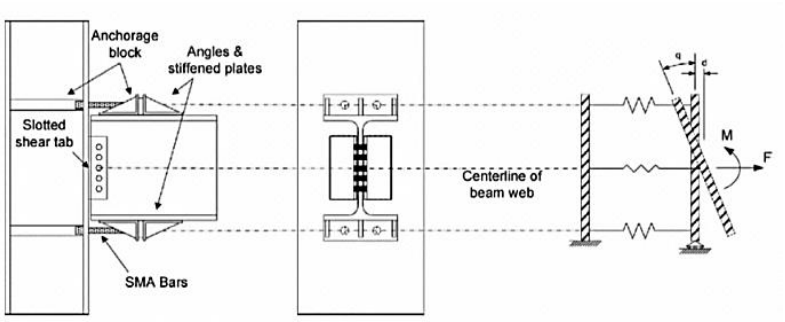

Figure 5. The connection model including SMAs provided by [12]

The beam column connections in steel frames with two elements containing SMA rod with large diameters, Figure 5. using superelastic SMA elements with the capability of being self-centering and elements of martensite SMA with the capability of high energy dissipation ,encounter with seismic vibrations has been evaluated. For this purpose two large steel structures (3 & 9 stories) were applied and capabilities of optimized connections with SMAs tested. Various testing showed that connections equipped with energy dissipation SMAs turned out to be more effective on the maximum displacement, while superelastic SMAs performed better in controlling residual displacement of structure[13]. The seismic performance of a variety of steel structure with various stories with SMA connections with focusing on rotational behavior of connections has been studied [14]. Hysteresis performance of T-shaped plate connection and bolts containing SMAs have been tested and found out that they had proper capabilities of self-centering and energy dissipation [15]. The innovative connection containing end plates and bolts of SMAs, continuity

plates, flange stiffeners, and web stiffeners has been studied. This connection turned out to have appropriate seismic performance, since its need for energy loss and ductility is provided with the transformation of shape memory bolts and thus the internal plastic hinge is formed, while structural parts mainly remain fixed within the elastic scope [16]. This issue was studied in detail. Studying on rotational performance of the end plate connections that are connected using bolts of high strength steel and SMAs. Figure 6. indicates that the SMAs connections showed great self-centering capability and applicative energy dissipation capacity with vibration absorption of up to %17.5. The common end plate Connection with high strength bolts showed that it offered an appropriate capacity for energy dissipation and ductility, but its rotational displacement was permanent. Moreover, in the SMA bolted connection, all the end plates function as a thick plate and no non-elastic displacement was observed in the plate. When the length and diameter of connection bolt was studied, thin bolts (long bolts with small diameter) showed higher ductility and better hysteresis stability [17].

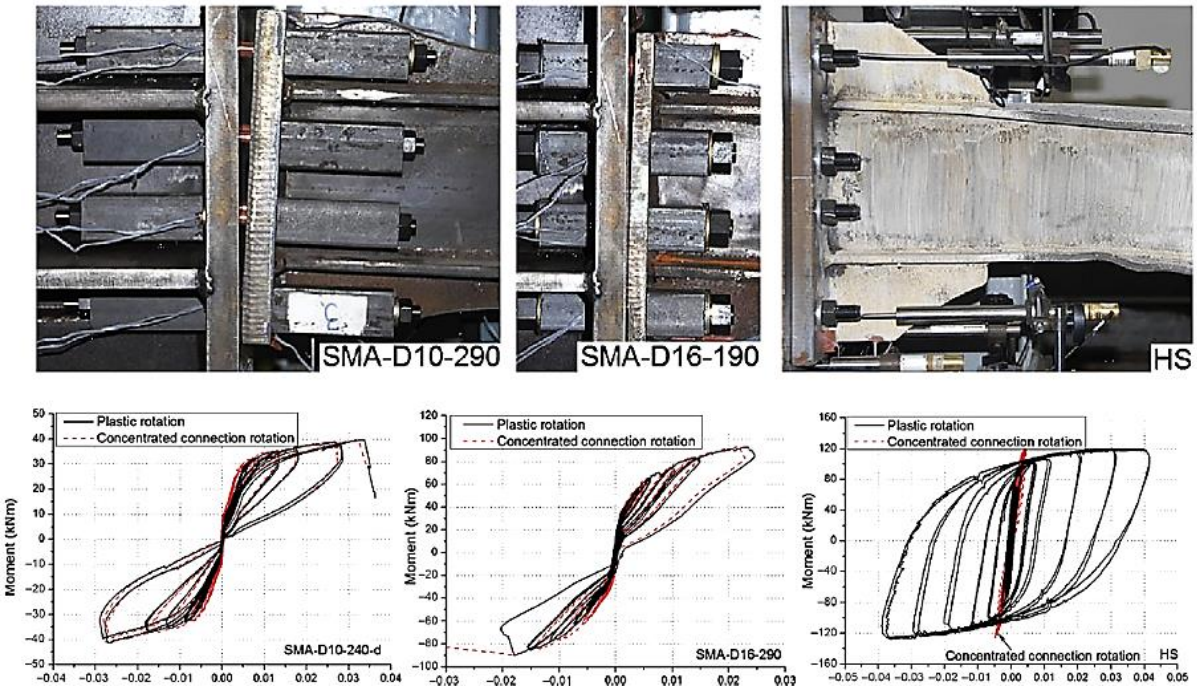

Figure 6. The connection model containing SMA bolts offered by [17]

4. The Sensitivity of MRF to Column Foundation Connections

The one span and one bay MRF and its geometry and dimensions, shown in Figure 7. was studied. Connection of column foundation is a torsion spring with the rotational stiffness of K_θ. The changes in the stiffness of torsional spring from $K_\theta = 0$ to $K_\theta = \infty$ resulted in hinged and restraining connections respectively. With the fixed concentrated mass the changes in the period of the structure were measured according to the rotational stiffness of the springs, and response of base shear affected by Tabas and Elcentro earthquakes, measured and the results were shown in Figure 7.

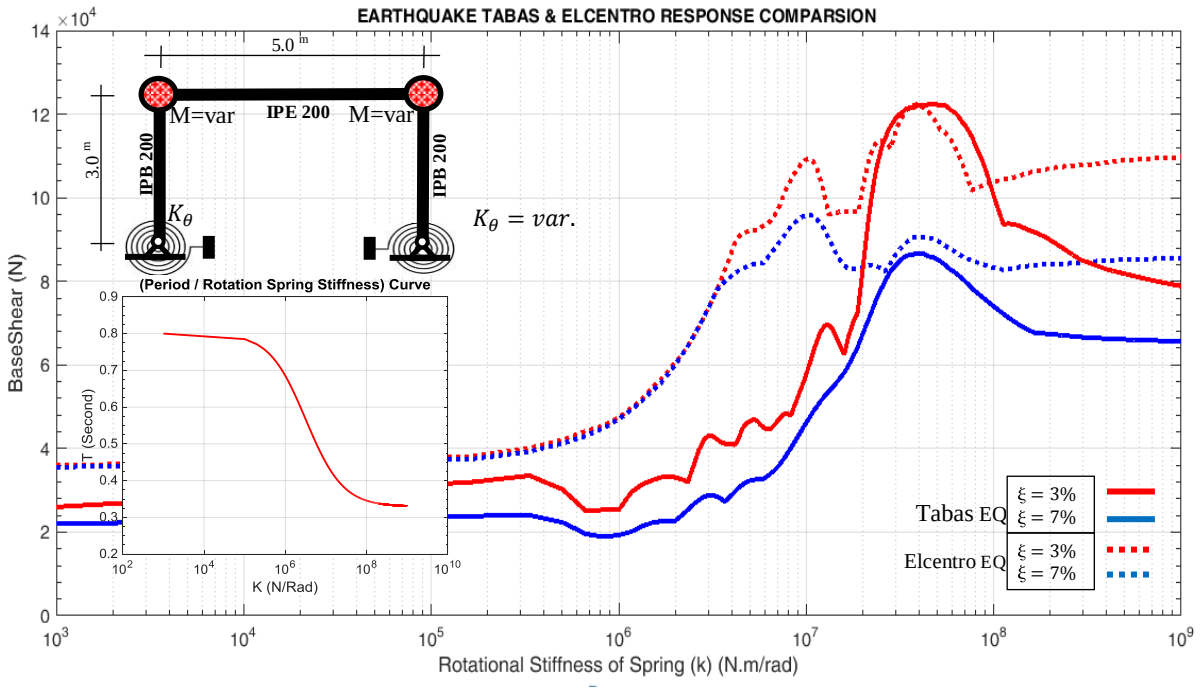

Figure 7. The general model of frame with spring connection (torsional) and rotational stiffness of K_θ and the changes in periods according to the rotational stiffness of K_θ and comparing the shear base spectrum for changing of rotational stiff of K_θ, under the earthquake records of Tabas and Elcentro

With respect to the changes of period as a function of connection stiffness (the presence of considerable changes in the period of 0.3 to 0.8 second, changes equal to nearly three times as the former) as well as the shear base spectrum (shown in Figure 10.) and its changes based on connection stiffness from 25 ^{KN} to 70 ^{KN} (nearly three times) for the earthquake with the damping of %7, the sensitivity of MRF to the column foundation connection method was quite obvious.

5. The Innovated Column Foundation Connection and Its Micro/Macro Behavior

The schematic view of fixed column foundation connection in Figure 8. is considered. It is assumed that the axial strain and stress caused by axial force in the column is tolerated by the base plate and foundation, where the column can rotate as the moment on the column at the support zone which is tolerated by the couple in the tie rod shown on the Figure 8. Assuming an IPB profile for the column and use of different materials for columns and rods as well as plastic entire cross section of the column, the equivalent diameter of rods Φ_{bar} can be calculated for replacement with the column to handle the incoming moment according to Equation 2.

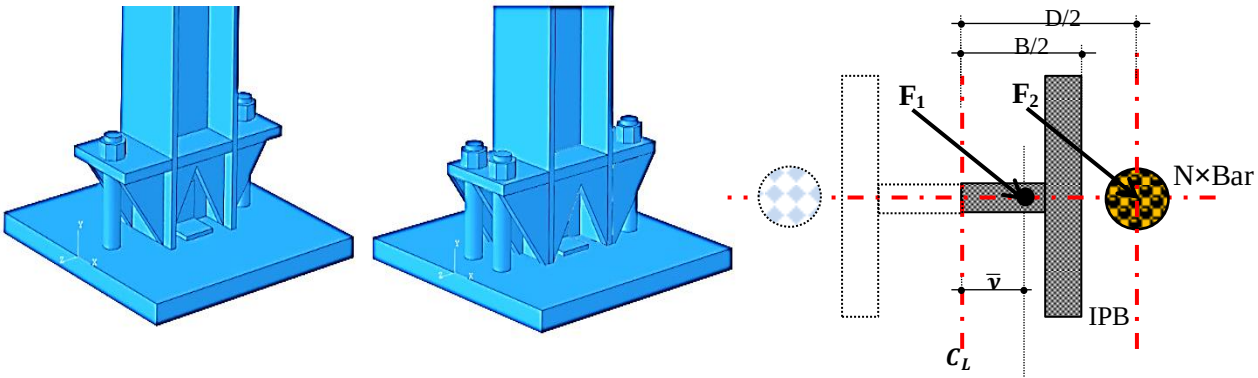

Figure 8. The schematic model of the connection (with 1 and 2 connection bars on both sides of the column) and parameters of connecting , connection bars and column profile

$$F_1 = \frac{1}{2} A_{IPB} \times \sigma_{y_{IPB}} \qquad \& \qquad F_2 = N \times A_{Bar} \times \sigma_{y_{Bar}} \tag{1}$$

$$\Phi_{bar} = \sqrt{\frac{8}{\pi \times N \times D} \times \frac{\sigma_{y_{IPB}}}{\sigma_{y_{Bar}}} \left[(\frac{B}{2} - t_f)^2 \times t_w + 2 \times (\frac{B}{2} - t_f) \times (b_f . t_f) \right]} \tag{2}$$

Where the parameters include:

Φ_{bar} = Equivalent rod diameter.
σ_{yBar} = Rod yield stress.
B = Height of IPB.
b_f = Width of profile flange (IPB).
t_w = Thickness of profile web (IPB).
A_{bar} = Rod cross-section.
N = Number of on each side.
D = Height of IPB plus distance between rod and flanges.
t_f = Thickness of profiles flanges (IPB).
σ_{yIPB} = Profile yield stress (IPB).

The Φ_{bar} for a few profiles can be obtained from Table 1. based on IPB and in terms of number of rods needed for different types of steel according to Equation 2, diameters of equivalent rods.

Table 1. Equivalent diameters of rods for IPB (made of different materials)

IPB	Φ_{bar} (mm)								
	$\sigma_{y_{Bar}} = 240\ mpa$			$\sigma_{y_{Bar}} = 300\ mpa$			$\sigma_{y_{Bar}} = 640\ mpa$		
	N_{bar}			N_{bar}			N_{bar}		
	2	3	4	2	3	4	2	3	4
160	28	23	20	25	20	18	18	14	12
180	31	26	22	28	23	20	20	16	14
200	35	29	25	31	26	22	22	18	16
220	39	31	27	34	28	24	24	20	17

5.1. Control of Column Buckling

The free length of the rod before buckling can be calculated in terms of diameter and materials according Euler differential Equation 4. and behavior of compressive and tensile performance of rods can be changed in moment direction.

$$\sigma_{cr} = \frac{\pi^2 E}{\left(\frac{KL}{r}\right)^2} \quad \& \quad \left(A = \frac{\pi D^2}{4} \quad \& \quad I_z = I_y = \frac{\pi D^4}{64} \quad \& \quad r = \sqrt{\frac{I_z}{A}} \quad \& \quad K = 1\right) \tag{3}$$

$$\sigma_{cr} = \frac{\pi^2 D^2 E}{16L^2} = \frac{\pi^2 E}{(\frac{4L}{D})^2} \tag{4}$$

By drawing Equation 4. (L/D & σ_{cr}) and taking yield stress limit $\sigma_y = 240\ Mpa$ into account and the elastic modulus $= 210\ Gpa$, the ratio L/D was obtained according to Figure 9 (a) for different types of steel with different σ_y and diameter depending on length, according to Figure 9. (b).

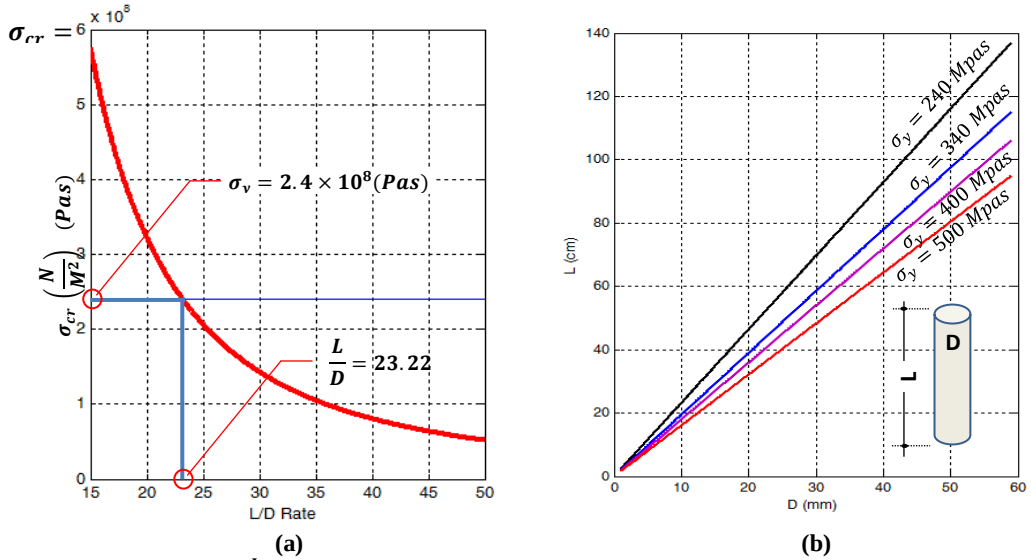

(a) **(b)**

Figure 9. (a) ratio $\frac{L}{D}$ for steel $\sigma_y = 240$ Mpa, E $= 210$Gpa , (b) D and L of steel rods with different σ_y

5.2. Control of Micro/Macro Behavior of Connection

Considering $B = 20\ cm, D = 35\ cm, H \approx 10\ cm, L = 10\ cm, Hc = 3.0\ m$, and the column profile being *IPB200*, and supposing the usage of two bars on two sides of the connection, $N = 2$. By using the Equation 1. and measuring the diameter of the bars $\Phi_{bar} = 35\ mm$, and the modeling of the connection both as micro and macro using OpenSees software (for macro model) and ABAQUS (for micro model) according to Figure 9. and conducting pushover analysis, the comparing of analysis findings for the base shear and the axial force of the bars (as indicated in Figure 10.) showed a similar behavior of both.

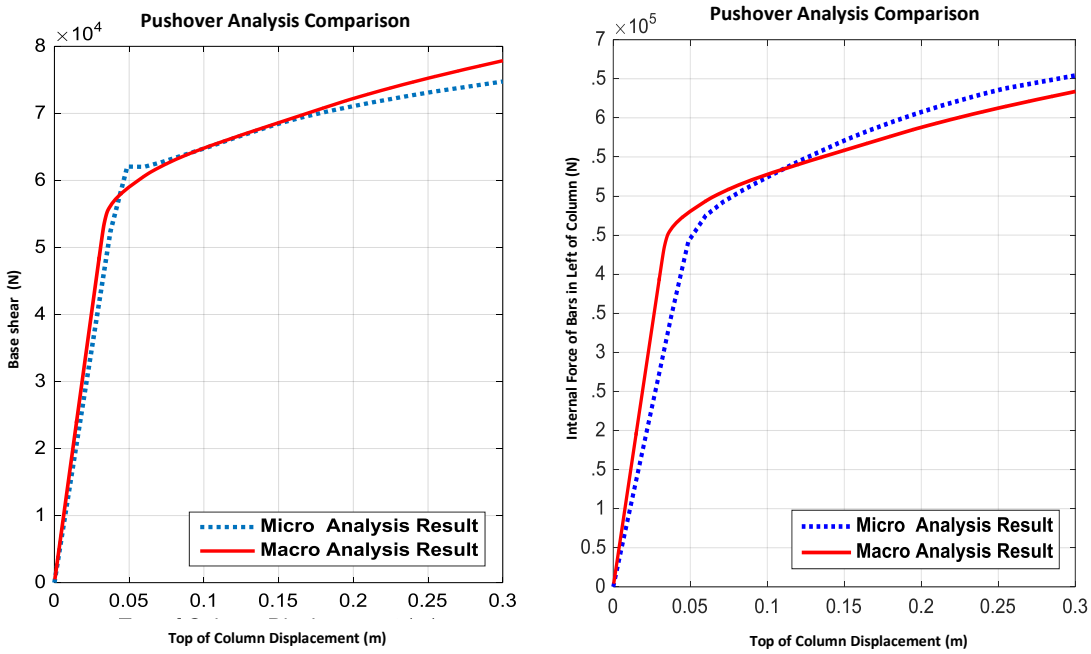

Figure 10. The comparison of pushover analysis in both micro and macro

5.3. Equipping the Connection with SMA

The steel bars were removed from the connection and superelastic Nitinol SMA bars were used instead. For this purpose the behavior of the superelastic SMA, Figure 11. was compared with similar performance in elasticity and compression.

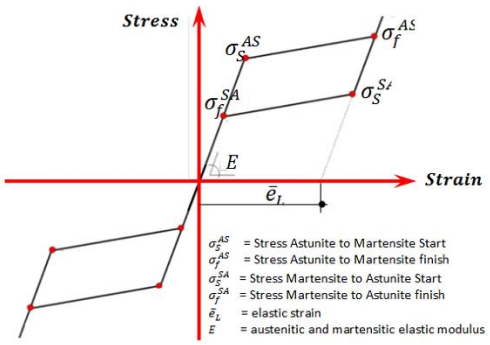

Figure.11 Superelastic stress-strain curve for NiTi SMArods

5.3.1. Verification of Connection Bars Performance

For verifying the performance of superelastic bars, used the experimental testing results obtained by Desroches, McCormick and Delemont, on the superelastic capability of Nitinol SMA wires and bars [18]. The samples tested specifications and the loading protocol and the test results were shown in Figure 12. For modeling, OpenSees was applied and the tested bar and results obtained from OpenSees and experimental test results were compared, and the results of which were shown in Figure 13.

Property	NiTi SMA	
	Austenite	Martensite
Physical properties		
Density	6.45 g/cm^3	
Mechanical properties		
Recoverable elongation	up to 8%	
Young's modulus	30–83 GPa	21–41 GPa
Yield strength	195–690 MPa	70–140 MPa
Ultimate tensile strength	895–1,900 MPa	
Elongation at failure	5–50% (typically 25%)	
Poisson's ratio	0.33	
Chemical properties		
Corrosion performance	Excellent (similar to stainless steel)	

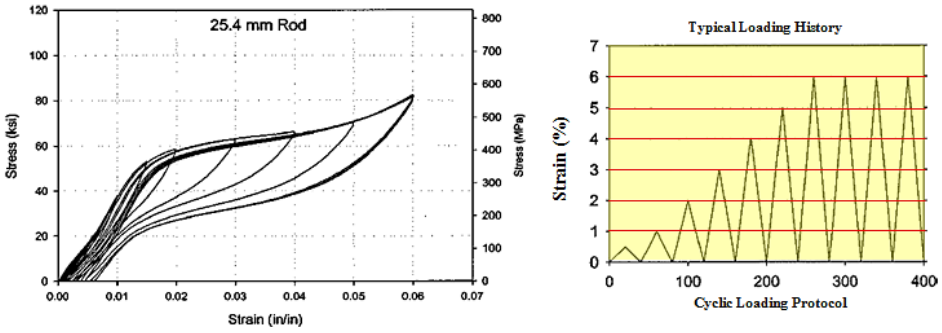

Figure 12. The comparison of laboratory findings obtained by [18]

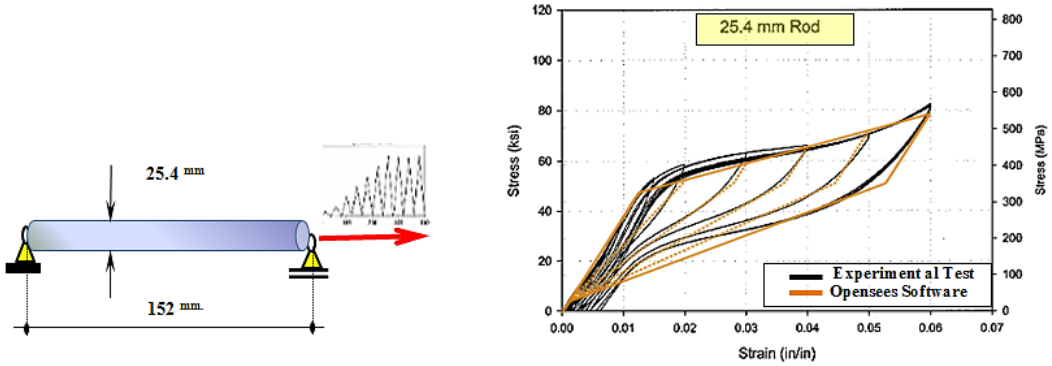

Figure 13. Comparison of experimental testing results obtained by [18] and OpenSees results

6. Performing the Test and Numerical Study of the Sample MRF

To performing the test as well as numerical study of steel MRF, one story and one bay steel frame were studied. First MRF was designed and then connection with steel bars designed and finally connection equipped with SMA bars was designed and finally performance of MRF with/without SMA bars was investigated.

6.1. Design of MRF Based on Iranian Codes (NIBC and 2800)

The live and dead loads as well as the combination of the loads were determined based on the sixth section of National Iranian Building Code(NIBC) , and its designing was conducted according to Iranian Earthquake Code 2800 (fourth edition, 2015). The geometric specifications, loading considerations, and factors of Code 2800 are shown in figure 14, and the result of frame design was shown in Figure 15.

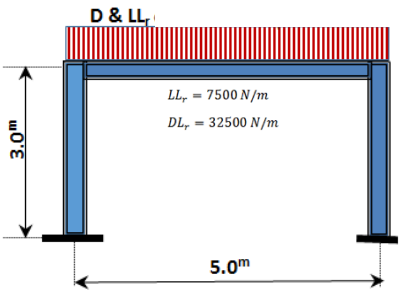

Factors of Iranian Earthquake code 2800						General Specification and Situation of Structure
$C = MAX(\frac{A.B.I}{R_u}\ \&\ 0.12A)$	$0.12A$	$\frac{A.B.I}{R_u}$	R_u	$B = B_1 \times N$ $B_1 = S_0 + (S - S_0 + 1) \times (T/T_0)$ $0 < T < T_0$ $B_1 = S + 1$ $T_0 < T < T_s$ $B_1 = (S + 1) \times (T_s / (T)$ $T > T_s$ $N = 1.0$ $T < T_s$ $N = \frac{0.7}{4 - T_s}(T - T_s) + 1.0$ $T_s < T < 4.0_{sec}$ $N = 1.7$ $T > 4.0_{sec}$	$T = \frac{80^{0.75}}{100}$	
0.175	0.042	0.175	5.0	$B_1 = 2.50$ $N = 1.0$ $B = 2.50$	0.1824	$A = 0.35$ $I = 1.00$ $T_0 = 0.10$ $T_s = 0.50$ $S = 1.50$ $S_0 = 1.00$ $H = 3.00^m$

Figure14. The geometric specifications, loading considerations, and Factors of Code 2800 in the studied MRF

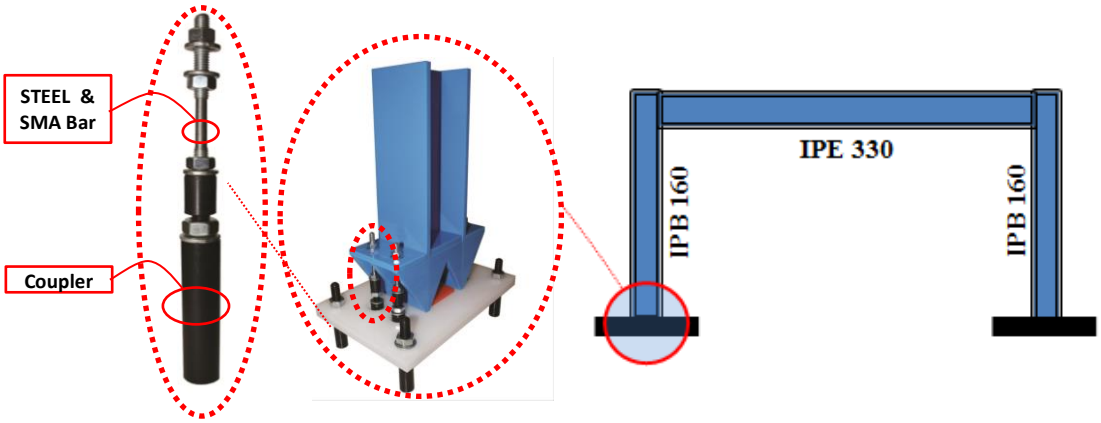

Selected Nitinol Shape Memory Alloy (SMA) Specification			
Mechanical Specification		Phase (Aus. To Mar.)	Phase (Mar. to Aus.)
Elasticity Mud. (E)		60 GPa	60 GPa
Stress	Start	250 MPa	150 MPa
	Finish	400 MPa	50 MPa
Elastic Strain		6%	6%

Figure 15. Designing result of MRF with innovated connection and specifications of selected SMA bars

6.2. Modeling of Frame and Connection in OpenSees and Considerations

The general model of the MRF with innovated connection were coded in OpenSees and for conducting the comparison of responses, the acceleration record scale factor ,as shown in Table 2. was measured according to Code 2800. The MRF was analyzed by using of Tabas, Elcentro, Luma , Kobe and Northridge earthquake records Figure 16. in two states: once under the scaled records; and the next time unde non scaled record of earthquakes Luma and Northridge, for comparing the performance. The effect of P-Δ was considered in the analysis and $\xi = 5\%$ was determined. Each time the structure was analyzed in two states of column foundation connection: once it included the innovated connection with steel bars; and the second time it was equipped with SMA bars (with the supposed specifications of the bars as shown in Figure 15. and with the selection of diameter and length in trial and error method, and buckling control according to Figure 9.).

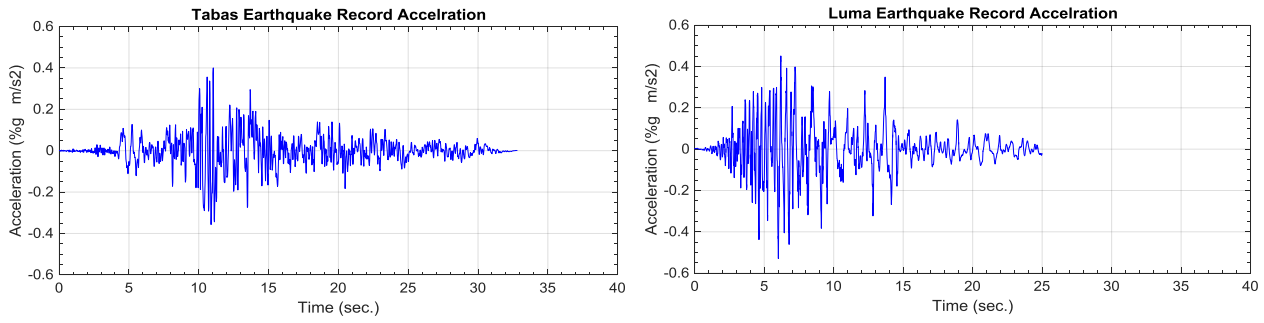

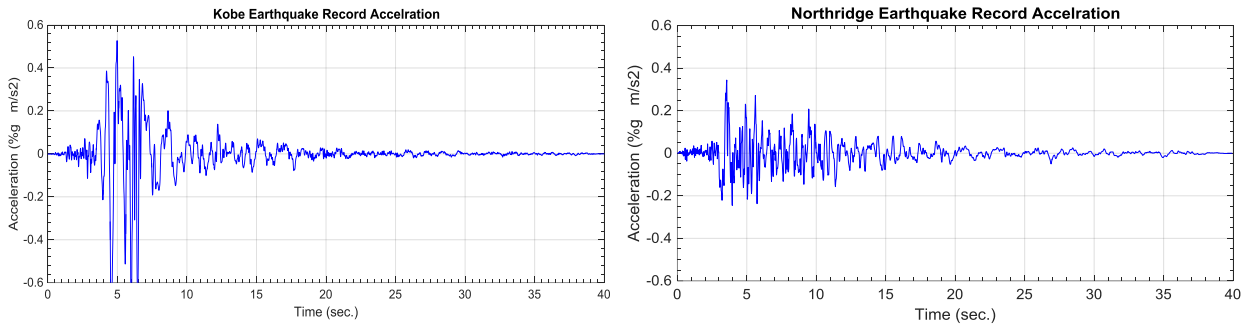

Figure 16. The acceleration Records of Tabas, Elcentro, Loma, Kobe, and Northridge earthquakes

Table 2. The scale Factor for selected earthquakes based on the recommendation of Iranian EQ Code 2800 (fourth edition)

Scaling Factor of Acceleration Recorde due to Iranian EQ code (2800)															The Studied Frame Specification				
Northridge (EQ)			Tabas (EQ)			Elcentro (EQ)			Luma(EQ)			Kobe (EQ)							
$f_1.f_2$	f_2	f_1	$f_1.f_2$	f_2	f_1	$f_1.f_2$	f_2	f_1	$f_1.f_2$	f_2	f_1	$f_1.f_2$	f_2	f_1	T Sec	T_m Sec	T_a Sec	Story	Bay
0.51	0.175	2.90	0.40	0.16	2.50	0.38	0.152	2.50	0.35	0.185	1.89	0.26	0.25	1.01	0.2279	0.39	0.1823	1	1

7. Response Results of MRF with/without SMA Bars Connection

The responses obtained are shown in the analysis state under the scaled records in Figures 17 and 18.

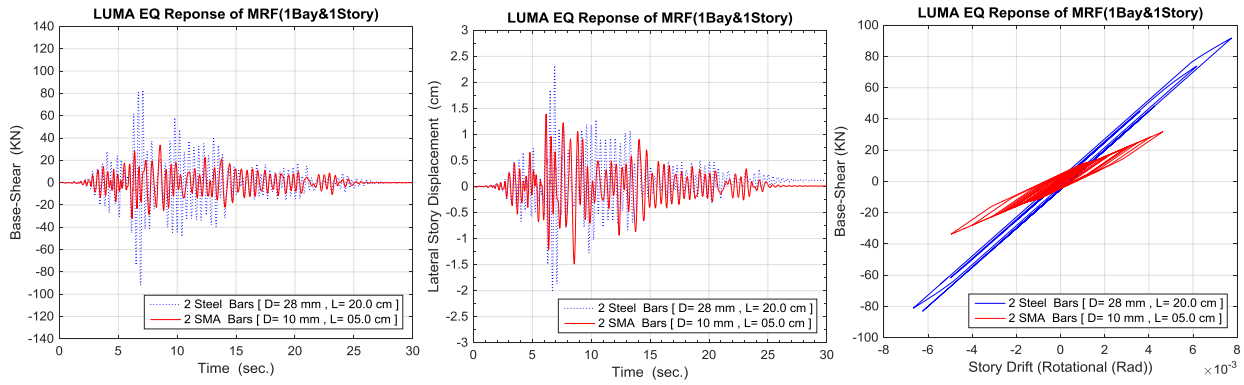

(a) - Time history of Base Shear (b) - Time history of lateral Displacement of roof (c) - Hysteresis of base shear–drift of the floor

Figure 17. Responses Results of studied MRF contained an innovative connection with/without SMA under the scaled record of earthquake of Loma

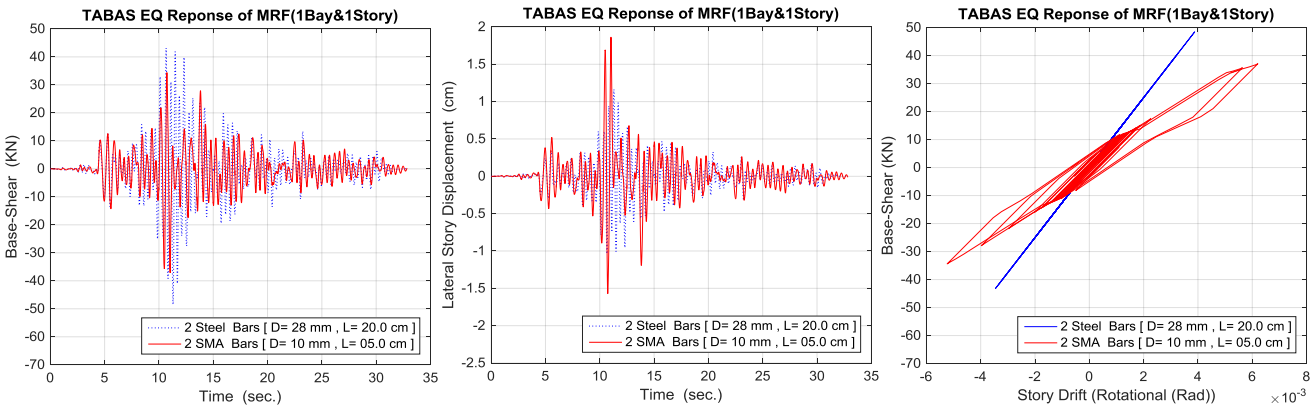

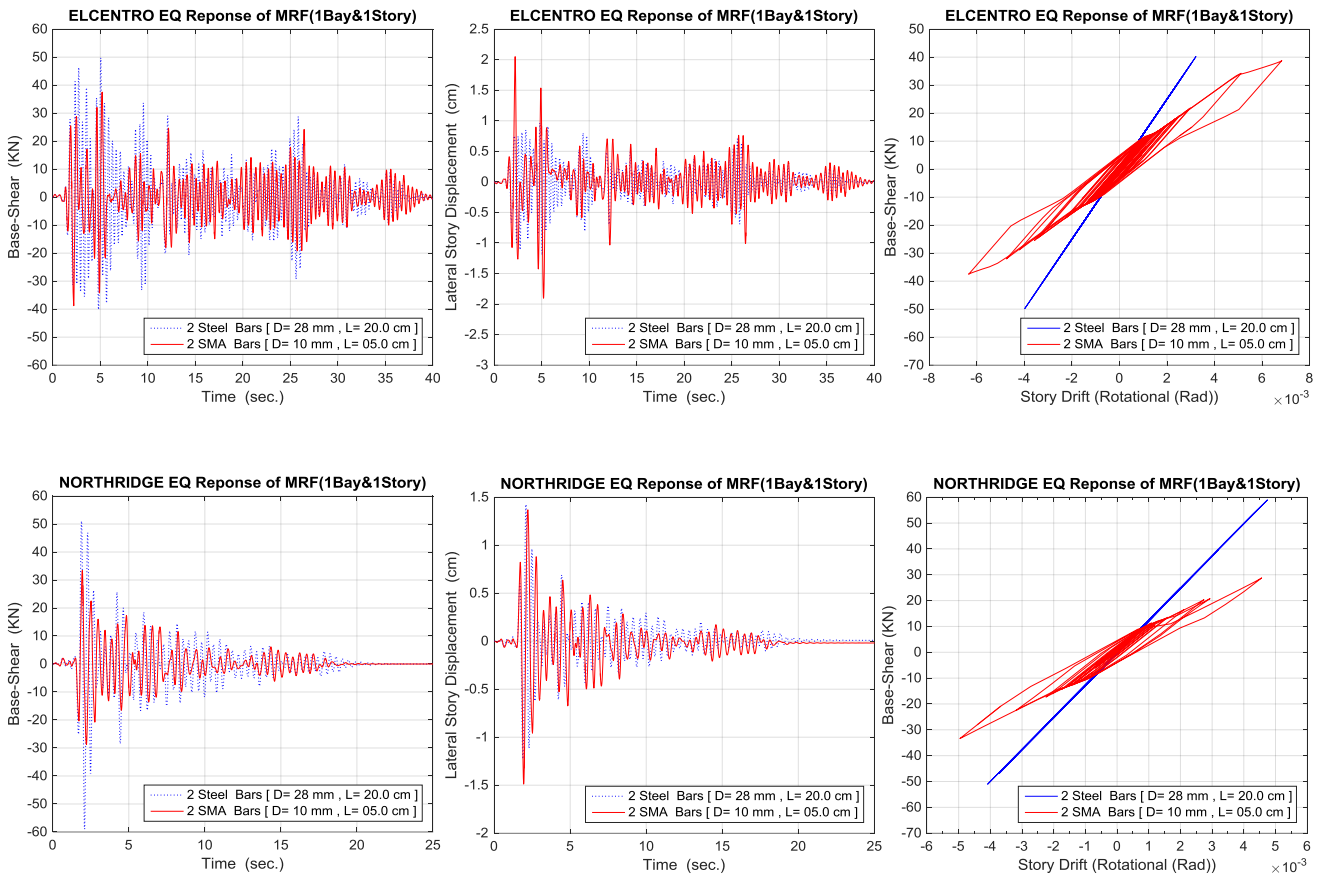

(a) - Time history of Base Shear (b) - Time history of lateral Displacement of roof (c) - Hysteresis of base shear–drift of the floor

Figure 18. Responses Results of studied frame contained an innovative connection with/without SMA under the scaled EQ record of Tabas, Elcentro, Northridge, Kobe

By analyzing the MRF through direct application of record to structure (non-scaled acceleration record) the records of Loma and Northridge earthquakes, the findings of the frame response were shown in Figure 19.The total result of responses are indicated in Table 3.

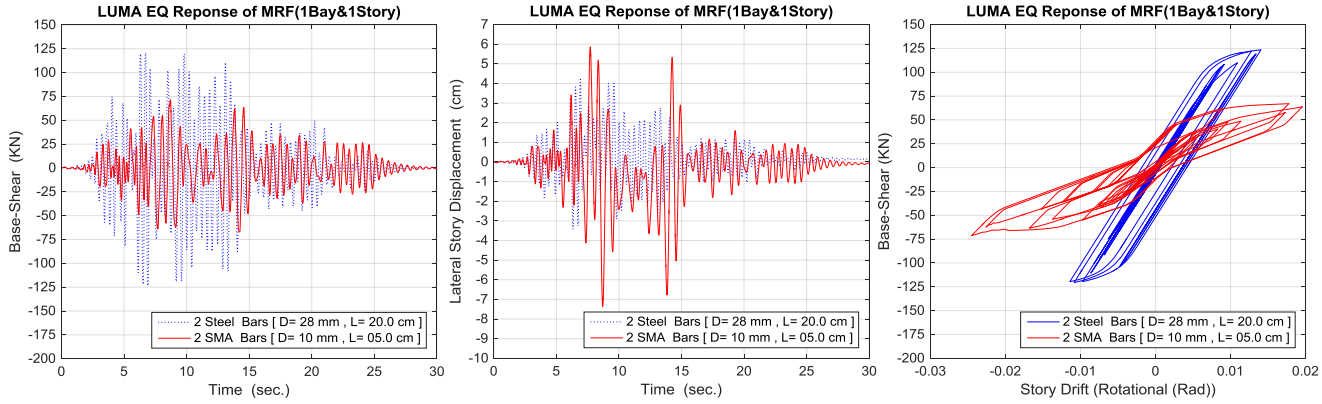

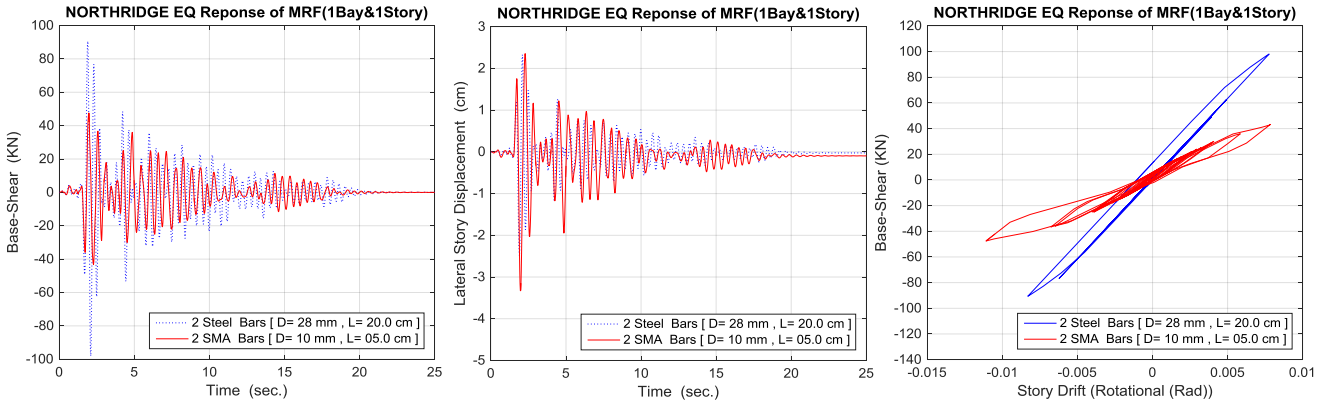

(a) - Time history of Base Shear (b) - Time history of lateral Displacement of roof (c) - Hysteresis of base shear–drift of the floor

Figure 19. Responses Results of studied frame contained an innovative connection with/without SMA under un-scaled earthquakes of Luma and Northridge

Table 3. Comparison response of studied MRF containing innovative connection (with/without SMA)

Dynamic Nonlinear Analysis with P-Δ effect					
Equipped with SMA Bars		Equipped with Steel Bars			
Absolute Roof-Disp. Δ_{max} (cm)	Absolute Base-Shear V_{Max} (KN)	Absolute Roof-Disp. Δ_{max} (cm)	Absolute Base-Shear V_{Max} (KN)	Selected Earthquake	Acceleration Record
1.4	31.9	2.3	91.9	Luma	Scaled
1.8	37.1	1.2	48.5	Tabas	
1.5	33.4	1.4	58.8	Northridge	
3.6	54.20	1.7	76.4	Kobe	
2.0	38.7	1.1	50.0	Elcentro	
7.7	70.2	4.2	123.1	Luma	Non-scaled
5.7	71.4	2.8	107.2	Tabas	
3.3	48.6	2.4	98.1	Northridge	
16.9	136.2	14.8	144.1	Kobe	
6.8	93.9	3.4	114.8	Elcentro	

8. Conclusion

- The suggested model for connecting the steel column to foundation enjoyed a real-life performance and offered acceptable results in both micro/macro analyses.
- With respect to the conformity of macro model with the conducted mode, the innovated connection is easily capable of being conducted, and the model in macro state can be used and conducted in the structure. The SMA equipped connection is easily macro modeled in software capable of analyzing SMA elements especially the bars.
- By studying the performance of SMA equipped connection, the self-centering capability arising from SMA elements is quite obvious, so that in none of the effective records on the structure and hysteresis diagrams residuary displacements are observed in the connection at the end of the analysis. This indicates the proper and effective performance of SMA equipped connection in self-centripetal performance.
- With respect to the performance of the connection as well as connection bars (when severe seismic excitations occur only the connection bars are likely to be damaged) and the possibility of fixing or replacing them, one can consider the aforementioned connection as one of the low-damage connections.
- The analysis findings of the frame containing connection equipped with shape memory alloys under scaled record indicate that although it keeps maximum displacement extent for most of the earthquakes used at an authorized scope, it reduces the base shear to a considerable extent.

- In studying analysis findings of the frame under the non-scaled record, although roof level displacement increased in all earthquakes, the effective base shear on the structure reduced considerably in all earthquakes. Moreover, although the increase in response of the lateral displacement and floor drift can apparently be a weak point of the connection, the findings obtained indicate that in comparing the displacement and residuary drifts in roof level, the residuary drifts in the structure containing connection equipped with SMA (in the last cycle and the completion of the free vibration in the structure) enjoyed a lower and (at times) authorized connection and this is due to its self-centering capability.
- The findings of the present study were considered for a particular bar with the supposed specifications. Since the connection is greatly dependent on the mechanical specifications (tensions in different phases, elasticity module, reversible strain) and engineering specifications (cross section and length), it is expected that better results to be achieved for the frame and connection performance by selecting appropriate mechanical specifications and optimizing the length and cross section for SMA bars.

9. References

[1] Aboozar Saleh, Seyed M. Zahrai and Seyed R. Mirghaderi, " Experimental study on innovative tubular web RBS connections in steel MRFs with typical shallow beams" Structural Engineering and Mechanics, An Int'l Journal 57(5) (2016):785-808.

[2] Qinghua Han, Mingjie Liu and Yan Lu, "Experimental research on load-bearing capacity of cast steel joints for beam-to-column" Structural Engineering and Mechanics, An Int'l Journal 56 (1) (2015): 67-83.

[3] Musa Artar and Ayse T. Daloglu, "Optimum design of steel frames with semi-rigid connections and composite beams" Structural Engineering and Mechanics, An Int'l Journal 55 (2) (2015): 299-313.

[4] Ertekin Öztekin, "Reliabilities of distances describing bolt placement for high strength steel connections" Structural Engineering and Mechanics, An Int'l Journal 54(1) (2015): 149-168.

[5] Leonardo Lecce and Antonio Concilio, eds. Shape Memory Alloy Engineering for Aerospace, Structural and Biomedical Applications. 1st Edition Elsevier Press Ltd, 2015.

[6] Ashwin Rao and A.R. Srinivasa J.N. Reddy , eds. Design of Shape Memory Alloy (SMA) Actuators. 1st Edition Springer Press, 2015.

[7] A. Sarvghad Moghadam, M. Nekooei, R. Jamalpour, ed. Optimal Design of Equipped Tuned Mass Damper (TMD) with Shape Memory Alloy (SMA) in Larg Span Steel Structure for Their Seismic Response Reduction and Control: Proceedings of the 3th International (ICSAU). Shahid Beheshti University ,Tehran ,Iran , 2015.

[8] Jamalpour Saeed ,Jamalpour Reza "The Shape Memory Alloys (SMA) Introducing and Evaluation of their Performance in Bending Moment Frame Connections" Journal of Current World Environment Special-Issue 133 (2015): 253-259

[9] Leon RT, DesRoches R, Ocel J, Hess G, Liu S. "Innovative beam column connections using shape memory alloys" Smart Syst Bridg Struct Highw 4330(2001):227-37 .

[10] Ocel J, DesRoches R, Leon RT, Hess WG, Krumme R, Hayes JR, "Steel beam-column connections using shape memory alloys" Journal of Structural Engineering ASCE 130(5) (2004):732-40.

[11] Sepulveda J, Boroschek R, Herrera R, Moroni O, Sarrazin M.(2008) "Steel beam-column connection using copper-based shape memory alloy dampers" Journal of Construction Steel Research 64(4) (2008): 429-35.

[12] Speicher MS, DesRoches R, Leon RT "Experimental results of a NiTi shape memory alloy (SMA)- based recentering beam-column connection" Engineering Structure 33(9) (2011): 2448-57.

[13] Desroches R, Taftali B, Ellingwood BR "Seismic performance assessment of steel frames with shape memory Alloy connections. Part I analysis and seismic demands" Journal of Earthquake Engineering 14(4) (2010): 471-86.

[14] Rofooei FR, Farhidzadeh A, "Investigation on the seismic behavior of steel MRF with shape memory alloy equipped connections"Proceeding of 12th East Asia-Pacific Conference of Structural Engineering Construction (EASEC12) 2011.

[15] Abolmaali A, Treadway J, Aswath P, Lu FK, McCarthy E. "Hysteresis behavior of t-stub connections with superelastic shape memory fasteners" Journal of Construction Steel Research 62(8) (2006): 831-8.

[16] Ma HW, Wilkinson T, Cho CD "Feasibility study on a self-centering beam-to-column connection by using the superelastic behavior of SMAs" Smart Material of Structure 16(5) (2007): 1555-63.

[17] Fang C, Yam MCH, Lam ACC, Xie L. "Cyclic performance of extended end-plate connections equipped with shape memory alloy bolts" Journal of Construction Steel Research 94(0) (2014):122-36.

[18] DesRoches R, McCormick J, Delemont M. "Cyclic properties of superelastic shape memory alloy wires and bars" Journal of Structural Engineering ASCE130(1) (2004): 38-46.